FUTURE PROSPECTS OF RF HADRON BEAM PROFILE MONITORS FOR INTENSE NEUTRINO BEAM[*]

Q. Liu[†], Case Western Reserve University, Cleveland, OH 44106, USA

M. Backfish, A. Moretti, V. Papadimitriou, A. V. Tollestrup, K. Yonehara, R. M. Zwaska, Fermilab, Batavia, IL, 60510, USA

M. A. Cummings, R. Johnson, G. Kazakevich, Muons, Inc., Batavia, IL 60510, USA

B. Freemire, Illinois Institute of Technology, Chicago, IL 60616, USA

Abstract

A novel beam monitor based on a gas-filled multi-RF-cavity is proposed to measure the precise profile of secondary particles for neutrino experiments. It promises to be radiation robust in extremely high-radiation environment. When a charged beam passes through a gas-filled microwave RF cavity, it produces electron-ion pairs in the cavity, which shifts the gas permittivity. The beam profile can thus be reconstructed from the signals from individual RF cavity built into the beam profile monitor. To help with the demonstration tests, the temperature dependence of the monitor and a new cavity geometry for the monitor are discussed.

INTRODUCTION

A novel beam monitor based on a gas-filled RF resonator is proposed to measure the precise profile of secondary particles downstream of a target in the LBNF beam line at high intensity. The RF monitor is designed to be radiation robust in extremely high-radiation environment. When a charged beam passes through a gas-filled microwave RF cavity, it produces electron-ion pairs in the cavity. The induced plasma changes the gas permittivity in proportion to the beam intensity. This permittivity shift can be measured by the modulated RF frequency and the quality factor. The beam profile can thus be reconstructed from the signals from individual RF cavity built into the beam profile monitor [1]. A demonstration test is underway, and the current results have shown technical feasibility. The next phase to validate the RF monitor concept consists of two steps: step (1) is to build and test a new multi-cell 2.45 GHz RF cavity that can be used for the NuMI beamline, and step (2) is to build and test a new multi-cell 9.3 GHz RF cavity that can be put in service in a future beamline at the LBNF for spatial resolution. Higher frequency makes smaller cavity and makes finer spatial resolution in the beam profile measurement, which is needed for LBNF. These two resonant frequencies are chosen since they are the standard frequencies for magnetron RF source.

One of the intrinsic issues on the RF monitor is the temperature increment due to the energy deposition of the incident beam. In order to promote increased accuracy in beam profile measurement, a new geometry of the cavity is considered, with simulation results supporting of its feasibility.

TEMPERATURE DEPENDENCE

As a particle beam is incident on and passes through the RF monitor wall, it deposits energy to the monitor. The mean stopping power can be obtained using the Bethe-Bloch formula. Assuming that all of the net energy deposition of the incident beam goes into Joule heating, this would create a temperature increment of the monitor. The rate of this energy deposition of the beam is defined as the beam power.

In order to see how this temperature increment would affect the monitor's performance, it is necessary to first find an analytic function that describes the behavior of the monitor's temperature. To simplify the problem, following assumptions are made:

- The main source of power input into the monitor is the beam power while the deposited power is removed by the natural convection of the room air.
- The beam profile is in the form of a delta function. That is to say that the beam distribution and particle interaction are not considered.
- The room of beam enclosure is treated as a heat reservoir, with constant temperature 300 K. This is critical for setting up the boundary condition later in the problem.
- The material properties of the cavity wall, such as the thermal and electrical conductivity, are independent of the temperature.

According to the assumption that the net energy deposition would all go into Joule heating, the following energy balance equation can be written:

$$P - hA[T(t) - 300] = cM\frac{dT(t)}{dt} \qquad (1)$$

where P is the power deposition by the incident beam, h is the heat transfer coefficient, A is the surface area of the monitor, c is the specific heat of the monitor wall, M is the total mass of the monitor, and $T(t)$ is the temperature of the monitor as a function of time, t.

The size of rectangular RF gas monitor is $20 \times 210 \times 10$ mm^3. It is made of aluminum, since it is a lightweight yet durable metal. Table 1 shows the parameters to evaluate Eq. (1) for each building material of the RF gas monitor. The major particle to deposit the energy is high energy protons. The average momentum of protons is 120 GeV/c in this calculation.

The first order linear differential equation produces asymptotic solutions, which will reach an equilibrium as time goes

Table 1: Parameters to Evaluate Eq. (1)

Material	dE/dx	h	c	M
Unit	MeV· cm^2/g	J/(kg· K)	kJ/(kg· K)	g
Aluminum	2.1324	10	0.9	47
Nitrogen	2.7828	10	1.04	0.073

to infinity. Figure 1 is an example when the beam intensity is 10^{14} particles/second, which is the case all primary proton beam strikes to a single RF cavity in the RF gas monitor by accident. The equilibrium temperature in this case is 431 K. The time constant is 243 s.
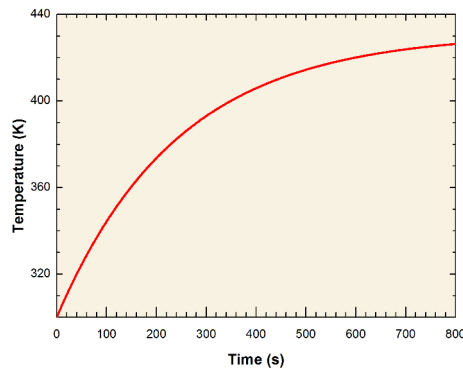
Figure 1: Time evolution of the monitor's temperature.

As the temperature of the monitor increases, its geometry change due to the thermal expansion. This has an effect on some of the monitor's parameters.

Equilibrium Temperature
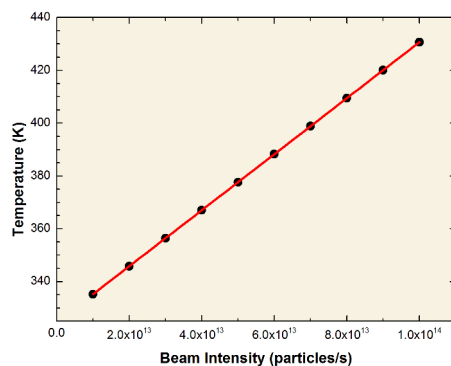
Figure 2: Equilibrium temperature of the monitor as a function of the beam intensity.

Figure 2 is obtained using Eq. (1) for various beam intensity values, and for each asymptotic solution, take the limit as the variable t goes to infinity to find the equilibrium temperature for that beam intensity. As can be observed in Figure 2, the equilibrium temperature grows linearly with respect to the beam intensity. The slope of the best-fit line

is 1.06×10^{-12} K/(particles/s). It uses the equilibrium temperature as the intermediate variable to build a crucial link between the beam intensity and all the other monitor parameters.

Frequency Shift
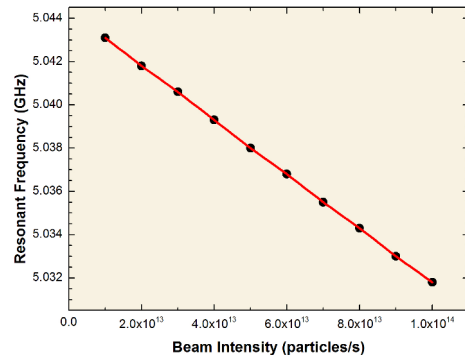
Figure 3: Resonant frequency of the monitor as a function of the beam intensity.

Each temperature increment corresponds to a geometry change, as the material experience thermal expansion. Using the information in Figure 2, the new dimensions of the resonator can be determined, and thus the new resonant frequency can be calculated. Figure 3 shows how the resonant frequency changes as a function of the beam intensity. The slope of the best-fit line is -1.26×10^{-16} GHz/(particles/s).

Surface Resistance
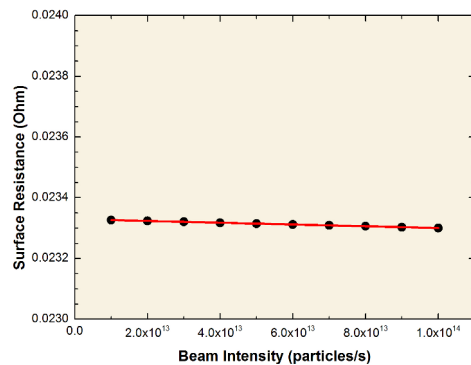
Figure 4: Surface resistance of the monitor as a function of the beam intensity.

The frequency shift would cause a change in the surface resistance. From Figure 4, we can conclude that the surface resistance does not vary much throughout the range.

Quality Factor Shift

Similarly, the unloaded quality factor can also be determined through the new geometry. The results can be found in Figure 5. From Figure 5, we can conclude that the quality factor does not change significantly throughout the range, staying relatively constant around 5160.

6: Accelerator Systems: Beam Instrumentation, Controls, Feedback, and Operational Aspects

T03 - Beam Diagnostics and Instrumentation
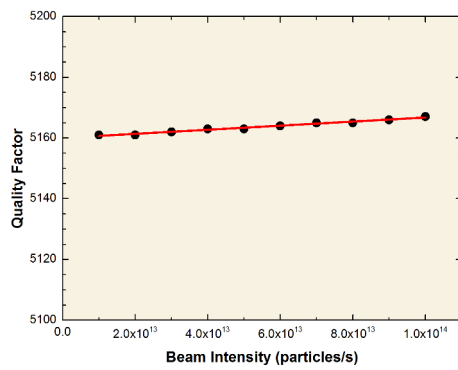
Figure 5: Quality factor of the monitor as a function of the beam intensity.

Gas Pressure
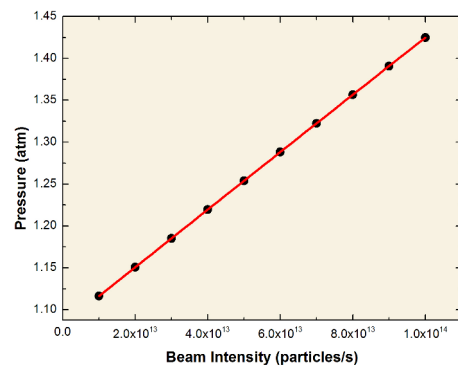
Figure 6: Gas pressure inside the monitor as a function of the beam intensity.

Finally, the gas pressure would change due to the temperature increment. For the initial state, we have nitrogen gas inside the RF monitor at 1 atmospheric pressure and room temperature. Using the van der Waals equation of state, the gas pressure can be found in this closed system. As can be seen in Figure 6, the gas pressure increases linearly with respect to the beam intensity. The slope of the best-fit line is 3.43×10^{-15} atm/(particles/s).

Now that these parameters can be specified for a given beam intensity, it is easier to control the system while performing the future demonstration tests.

CAVITY DESIGN

So far, a cylindrical-shaped RF cavity, commonly known as a pillbox cavity, is used to investigate feasibility of the RF gas monitor. A re-entrant RF cavity will be another possible cavity for the RF gas monitor. An excited electric field in a re-entrant cavity is concentrated in a narrow electrode gap. Hence, the excited magnetic field at the quarter RF period later is located outside of the electrode. This cavity translates to an equivalent resonant circuit that the
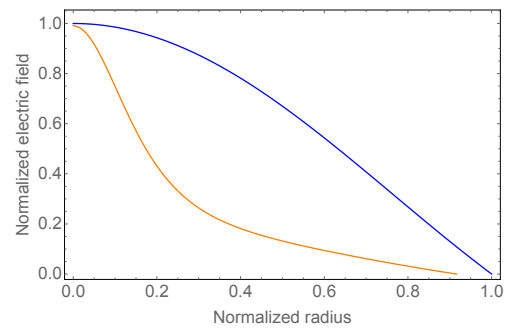
Figure 7: Simulated electric field map in a pillbox cavity (blue) and a re-entrant RF cavity (orange).

capacitance and inductance of the resonator are changed by altering resonator geometry. The radius of re-entrant cavity (R) decreases by increasing the capacitance (C) for a fixed resonant frequency, i.e. $R \propto 1/\sqrt{C}$. As a result, the size of re-entrant cavity is smaller than the pillbox cavity with a fixed resonant frequency. Figure 7 shows the excited electric field in a pillbox and re-entrant cavities at the fixed resonant frequency. Poisson Superfish is used to simulate the field map for the re-entrant cavity. Geometry of modeled re-entrant cavity is shown in reference [2].

There are two possible advantages of utilizing the re-entrant cavity for the RF gas monitor. First, the cavity is cost effective. The main driving cost of the RF gas monitor is the RF source. In general, the price of a GHz-band RF source is higher if it can produce higher driving frequency. The size of re-entrant cavity can be a half of the pillbox cavity with the fixed driving frequency. Second, the plasma loading in the re-entrant cavity will be lower than that in the pillbox cavity. The beam-induced plasma in a gas-filled RF cavity consumes RF power, which is called the plasma loading. Sometimes the plasma loading overloads the cavity, because all incident charged particles in the cavity contribute to the RF power consumption. It can be mitigated in the re-entrant cavity. The excited electric field is concentrated in the center of the cavity, and it is rapidly dropped with the radius by comparing the pillbox cavity as shown in Figure 7. If the incident charged particles uniformly distributes in the cavity the plasma loading (dW) is proportional to the square of the electric field ($E(r)$), i.e. $dW \propto \int E(r)^2 dV$. The plasma loading in the re-entrant cavity is six times lower than that in the pillbox one.

Two different shape cavities will be tested at Fermilab. The advantages of re-entrant cavity will be verified in experiment.

REFERENCES

[1] K.Yonehara *et al.*, in *Proc. IPAC2015*, pp. 1189-1191.

[2] B. Freemire *et al.*, "Pressurized rf Cavities in Ionizing Beams", *Phy. Rev. Acc. Beams 19*, 062004, 2016.